Journal of Engineering and Technology for Industrial Applications

ISSN ONLINE: 2447-0228

ITEGAM-JETIA

Manaus, v.11 n.56, p.382-390. November/December, 2025.

DOI: https://doi.org/10.5935/jetia. v11i56.2924

RESEARCH ARTICLE OPEN ACCESS

A NEW COMPUTATIONAL METHOD FOR THE INTERACTION BETWEEN CYLINDRICAL PERMANENT MAGNETS AND MASSIVE CIRCULAR COIL

Naamane Mohdeb[1], Hicham Allag[2] and Mohammed Chebout[3]

[1, 2]L2EI Laboratory, Mohamed Seddik Ben Yahia University, Jijel, Algeria.
[3]Applied Automation and industrial Diagnostic Laboratory, Ziane achour university, Djelfa, Algeria.

[1]https://orcid.org/0009-0000-7536-6435, [2]https://orcid.org/0009-0007-4787-3780, [3]http://orcid.org/0009-0006-2798-5411

Email: *mohdeb.naamane@univ-jijel.dz, hichamallag@univ-jijel.dz, mchebout@univ-djelfa.dz

ARTICLE INFO

Article History
Received: November 11, 2025
Revised: November 20, 2025
Accepted: December 1, 2025
Published: December 31, 2025

Keywords:
Cylindrical magnet,
Massive circular coil,
Magnetic interaction,
Amperian model,
Coulombian model.

ABSTRACT

A novel analytical method has been developed to accurately model the magnetic interaction between a massive circular current-carrying coil and cylindrical permanent magnets. This new approach, rooted in the coulombian model, addresses the computational complexity of cylindrical shapes by proposing a smart decomposition: the magnets are analytically partitioned into a grid of (N, M) elementary cuboidal magnets. This approximation not only calculates the magnetic force between two cylindrical magnets but also accurately models the forces between a coil and a magnet. Crucially, the method outperforms the modified filament technique and is demonstrably accurate, showing excellent agreement with measured values. The resulting simplified, yet highly accurate, calculation tool is ideal for the rapid design of advanced magnetics systems, including unconventional magnetic couplings and planar actuators.

I. INTRODUCTION

Several ironless magneto-mechanical devices used in electrical engineering require permanent magnets (PMs) and coils. We can take the example of magnetic levitation-based electromagnetic energy harvesting [1], ironless inductive position sensors [2], contactless energy transfer for a planar actuator [3], [4], and so on. Accurate calculation of magnetic interaction parameters is crucial for designing applications like eddy current dampers, magnetic refrigerators, and micropumps. These calculations are essential for determining forces, torques, and inductance in systems with moving parts or varying distances, ensuring predictable performance and efficiency. The Coulombian and Amperian models are two equivalent ways to describe the magnetic field of a permanent magnet. The Coulombian model treats a magnet as having magnetic poles that exert a force on each other, similar to electric charges, and uses a magnetic charge density to calculate the field. The Amperian model views a magnet as being made of microscopic current loops (Amperian currents) and uses these currents to determine the magnetic field. While different in their approach, they are mathematically equivalent and can be used interchangeably to calculate a magnet's field, though one may be simpler for certain geometries. The choice between the two often comes down to the geometry of the magnet and the specific problem being solved.

For example, the Amperian model can be useful for calculating fields from current loops, while the Coulombian model might be more intuitive for calculating the force between permanent magnets [5], [6]. Previous energy with research on the force between cylindrical permanent magnets often yielded complex and computationally expensive expressions. These methods typically relied on fundamental magnetostatic laws, integral equations or approximations. Such models are cumbersome because calculating the force is inherently complex, depending on the magnet's geometry, magnetization, and orientation. Many expressions published in previous literature [7-17] are criticized for: lack of exact Solutions, high Complexity, computational cost. Agashe et al [8] presented an analytical formula based on the assumption of uniform magnetization in the axial direction while using a magnetic field approximation for a cylindrical magnet [8]. These expressions are complex and computationally more expensive than the closed-form expression given by Furlani [9-11]. Researchers like Ravaud et al. [5], [6] provided formulas involving elliptic integrals without simplification for parameters

like field, force, torque, and stiffness, further highlighting the inherent complexity of the calculation. Calculating the force is recognized as a very complex procedure because it is highly dependent on the magnet's form, magnetization, and orientation. Many early exact formulas were incredibly lengthy, containing a double summation of nine terms, each involving these elliptic integrals and complex parameters. The majority of these works and others are based on the complete or simplified integral equations between magnets. Calculating the force is a very complex procedure, as it depends on the form, magnetization, and orientation of the magnets. To overcome these computational and complexity hurdles, the current work proposes a shift in modeling strategy:

- The use of the amperian current model is considered "more interesting" and suitable for deriving the new, simpler, and more efficient analytical expression.
- The goal is to present a new expression that is less complex and more computationally tractable than most previous works.

We aim to develop simpler, more computationally efficient analytical expressions for calculating the magnetic force in two specific configurations: between two cylindrical permanent magnets and between a cylindrical permanent magnet and a large, circular coil (solenoid). This approach is intended to be more effective than prior work that lacked exact solutions and was more complex. The expressions can be used to calculate the magnetic interaction between two cylindrical permanent magnets in a computationally efficient way. The paper introduces a new method for accurately calculating the magnetic force in two specific configurations: between two cylindrical permanent magnets and between a cylindrical permanent magnet and a large, circular coil (solenoid).

II. ELECTROMAGNETIC FORCE EXPRESSION

For specific geometries, such as the axial force between a thick coil and a permanent magnet or between magnets, more complex equations involving integrals are required. These equations incorporate the radii of the coil and the axial distance between them, as well as complete elliptic integrals. Calculating the force in practical scenarios usually involves advanced mathematics (e.g., elliptical integrals or numerical methods) because the magnetic fields are rarely uniform across the entire coil.

II.1 PERMANENT MAGNET MODEL

We generally use the Amperian current model or the coulombian approach [9-3] for calculating the magnetic field produced by PMs (Figure 1). We can say that the choice of the model does not depend on the magnetic source nature. Indeed, in the Coulombian approach, a magnetized magnet can be replaced by two charged surfaces, which are located on the lower and upper faces of this magnet. In the same way, a thin coil carrying uniform current density can also be represented by two charged planes. However, in the case of PM whose polarization is in tesla, its equivalent current must satisfy the following equation:

$$\vec{K} = \left(\vec{J} \times \vec{n}\right)/\mu_0 \tag{1}$$

Where n is the normal unit and μ0 is the permeability of the vacuum. This implies that a parallelepiped PM can be replaced by a thin coil whose current surface density is related to magnetic polarization J, as:

$$J = \mu_0 \frac{N.I}{h} \tag{2}$$

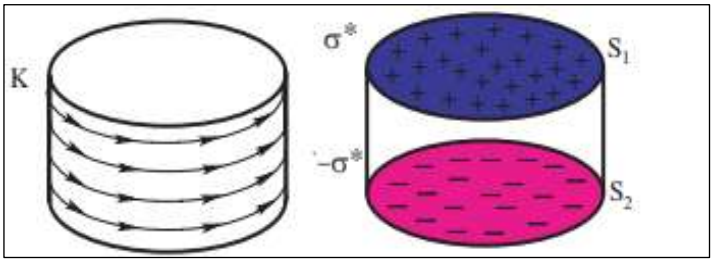

Figure 1: Representation of a cylindrical or cuboidal permanent magnet by Amperian current model and Coulombian approach.
Source: Authors, (2025).

II.2 MAGNETIC FORCE BY NUMERICAL DISCRETISATION TECHNIQUE

The Figure 2 on the right illustrates a numerical discretization technique, often used for modeling a uniform surface charge density. The idea in calculus is that while using a few rectangles gives a rough approximation, using an infinite number of infinitesimally thin rectangles gives us the exact area and, consequently, the exact electric field. In the figure, we are approximating the surface using inner rectangles (each rectangle is inside the curve). We can then find the region of each of these rectangles, add them up and this will be an estimate of the region. Using several rectangles will give us an exact approximation of the circular surface. The size of the rectangular elements is 2a x 2b, and “hi” is the center of each element.

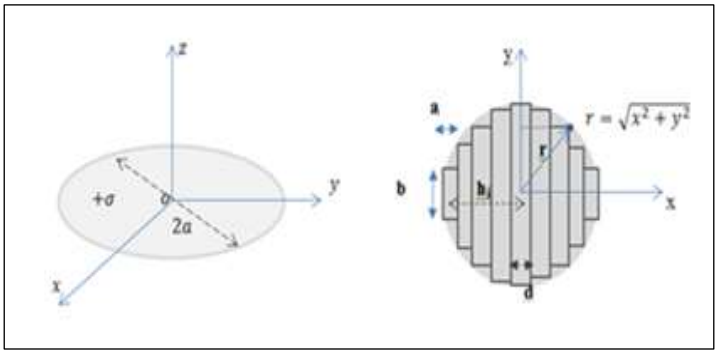

Figure 2: Decomposition of the circular surface
Source: Authors, (2025).

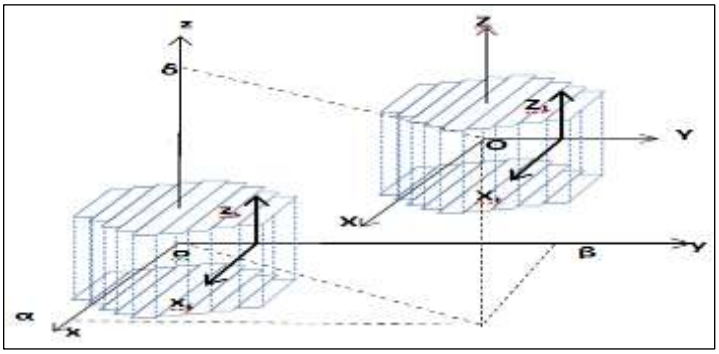

Figure 3: Elementary decomposition of cylindrical magnet
Source: Authors, (2025).

The modeling of magnets can be based on coulombian method, the coulombian approach replaces the magnet by two surfaces distribution of fictitious magnetic charge with surface density σ* = M. n. In Figure 3, the cylindrical magnet is to be replaced by a cuboidal shape composed of N cuboidal magnets. The interaction forces between the cylindrical magnets can be calculated by the following formula:

$$F_{magnet} = \sum_{s=1}^{N} \sum_{t=1}^{M} F_{s,t} \tag{3}$$

Where N and M are the number of a first and second elementary magnets, respectively. The interaction energy between two elementary magnets t and s, as shown in Figure 3, is given by:

$$E_{t,s} = \frac{J\,J'}{4\pi\mu} \sum_{p=0}^{1} \sum_{q=0}^{1} (-1)^{p+q} \cdot \int_{-B}^{B} \int_{-A}^{A} \int_{-b}^{b} \int_{-a}^{a} \frac{1}{R}\, dx\, dy\, dX\, dY \tag{4}$$

The components of force can be calculated by:

$$\overrightarrow{F_{s,t}} = g\overrightarrow{rad}(E_{s,t}) \tag{5}$$

With :

$$F_{s,t} = \frac{J\,J'}{4\pi\mu} \sum_{s=1}^{N} \sum_{t=1}^{M} \sum_{i=0}^{1} \sum_{j=0}^{1} \sum_{k=0}^{1} \sum_{l=0}^{1} \sum_{p=0}^{1} \sum_{q=0}^{1} (-1)^{i+j+k+l+p+q}\, \psi_{st(x,y,z)} \tag{6}$$

Where

$$\psi_{stx} = \frac{1}{2}\left(V_{st}^{\,2} - W_{st}^{\,2}\right) \ln(R_{st} - U_{st}) + U_{st} V_{st} \ln(R_{st} - V_{st}) + V_{st} W_{st} \arctan\left(\frac{U_{st} V_{st}}{R_{st} W_{st}}\right) + \frac{1}{2} R_{st} U_{st} \tag{7}$$

$$\psi_{sty} = \frac{1}{2}\left(U_{st}^{\,2} - W_{st}^{\,2}\right) \ln(R_{st} - V_{st}) + U_{st} V_{st}\, ln(R_{st} - U_{st}) + U_{st} W_{st}\, arctan\left(\frac{U_{st} V_{st}}{R_{st} W_{st}}\right) + \frac{1}{2} R_{st} V_{st} \tag{8}$$

$$\psi_{stz} = -U_{st} W_{st} \ln(R_{st} - U_{st}) - W_{st} V_{st} \ln(R_{st} - V_{st}) + U_{st} W_{st} \arctan\left(\frac{U_{st} V_{st}}{R_{st} W_{st}}\right) - R_{st} W_{sk} \tag{9}$$

The intermediate variables appearing in Eq. (9) are:

$$U_{st} = \alpha + (A\ \ (s+1) - 2i\, \Delta x2_s(s)) - (a\ \ (t+1) - 2j \Delta x1_t(t)) \tag{10}$$

$$V_{st} = \beta + (-1)^p B\ \ (s) - (-1)^l b\ \ (t) \tag{11}$$

$$W_{st} = \gamma + (-1)^q C\ \ -(-1)^k c \tag{12}$$

$$\Delta x1_s(s) = ((A\ \ (s+1) - A\ \ (s))/2 \tag{13}$$

$$\Delta x2_t(t) = ((a\ \ (t+1) - a\ \ (t))/2 \tag{14}$$

$$R_{st} = \sqrt{U_{st}^{\,2} + V_{st}^{\,2} + W_{st}^{\,2}} \tag{15}$$

II.2.1 Magnetic Force in Cylindrical Single Axis Actuator

The new approximation can also be used to evaluate the force between a massive circular coil and a cylindrical magnet (Figure 4). The force between a circular coil and a magnet is a result of the interaction between the magnetic field of the magnet and the magnetic field produced by the current in the coil. This force can be calculated by using the formula for the Lorentz force, which involves integrating the differential force along the wire of the coil. The total magnetic force acting on the thin coil is given by;

$$\overrightarrow{F_T} = \int_{V_c} \overrightarrow{J_c} \times \overrightarrow{B}\, dV_c \tag{16}$$

$$\overrightarrow{F_T} = \int_{V_c} \begin{pmatrix} Jx \\ Jy \\ 0 \end{pmatrix} \times \begin{pmatrix} B_{xt} \\ B_{yt} \\ B_{zt} \end{pmatrix} dX\, dY\, dZ \tag{17}$$

Where V_c is the volume of the bar-shaped volume. Jc is the current density in bar-shaped volume, and B is the field created by a cylindrical magnet.

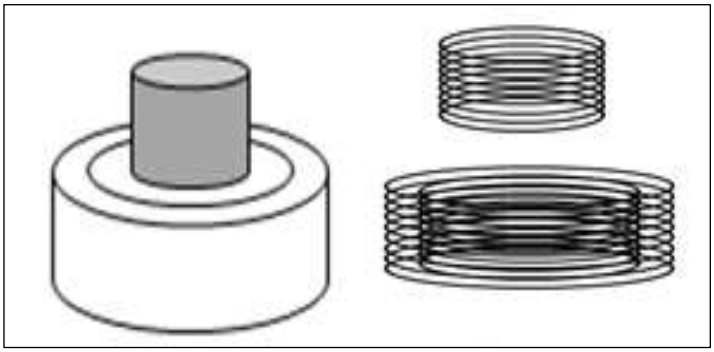

Figure 4: System composed of a permanent magnet.
Source: Authors, (2025).

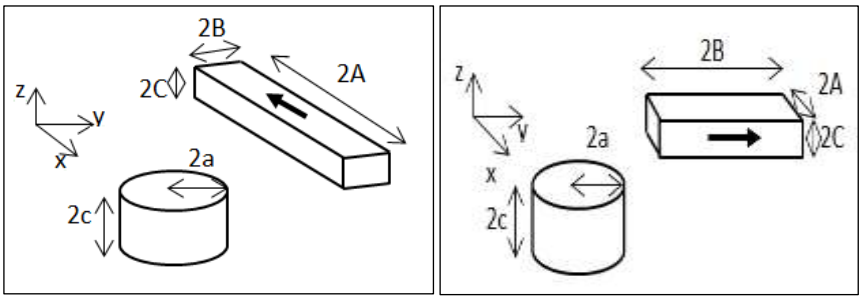

(a) (b)

Figure 5: PM and massive conductor in: a) x-direction , b) y-direction and thin coil.
Source: Authors, (2025).

By dividing the coil into four massive conductor, the model can precisely calculate the net useful force, the magnetic force has been obtained analytically. The force is derived for the bar-shaped volume shown in Figure 5, with volume current density J and dimension (2A x 2B x 2C). The coil moves in translation along the z-direction. The interaction force between the coil and the cylindrical magnet is given by:

- The current in x-direction:

$$F_y = -\frac{I}{CB}\frac{B}{4\pi}\sum_{t=1}^{M}\sum_i\sum_j\sum_k\sum_l\sum_p\sum_q(-1)^{i+j+k+l+p+q}\ \varphi_n \tag{18}$$

$$F_z = \frac{I}{CB}\frac{B}{4\pi}\sum_{t=1}^{M}\sum_i\sum_j\sum_k\sum_l\sum_p\sum_q(-1)^{i+j+k+l+p+q}\ \psi_n \tag{19}$$

- The current in y-direction:

$$F_x = -\frac{I}{CA}\frac{B}{4\pi}\sum_{t=1}^{M}\sum_i\sum_j\sum_k\sum_l\sum_p\sum_q(-1)^{i+j+k+l+p+q}\ \varphi_n \tag{20}$$

$$F_z = \frac{I}{CA}\frac{B}{4\pi}\sum_{t=1}^{M}\sum_i\sum_j\sum_k\sum_l\sum_p\sum_q(-1)^{i+j+k+l+p+q}\ \phi_n \tag{21}$$

These forces are obtained with the intermediate variables:

$$\varphi_n = \int\int\int arctg\left(\frac{VU}{WR}\right) dX\, dY\, dZ = \frac{R}{6}(U^2+V^2-W^2) + 6\,UVW\ arctg(\frac{VU}{WR}) - 3\,U\,(V^2-W^2)\ arctgh(\frac{R}{V}) - 3V(U^2 - W^2)\ arctgh(\frac{R}{V})) \quad (22)$$

$$\phi_n = \int\int\int \log(-V+R)\, dX\, dY\, dZ = \frac{1}{36}(-24\,U^3\ arctg\left(\frac{V}{U}\right) + 12\,V\,W\,R - 18\,U^2\,W\log(R+V) - 18\,U^2\,V\log(R+W) + 36\,U\,V\ \ W\log(R-U) + 18\,UW^2\ arctg\left(\frac{UV}{WR}\right) + 18\,U\,V^2 arctg\left(\frac{UW}{VR}\right) + 6W^3 log(R+V) + 6\,V^3 log(R+W) + 24\,U^2V - 6\,U^3\ arctg\left(\frac{VW}{RU}\right) + 18UV^2\ arctg\left(\frac{W}{V}\right) + 36\,U\,W^2 arctg\left(\frac{V}{W}\right) + 18\,U\,W^2 arctg\left(\frac{W}{V}\right) - 54\,U\,V\,W - 2V^3) \quad (23)$$

$$\psi_n = \int\int\int \log(-U+R)\, dX\, dY\, dZ = \frac{1}{36}(-24\,V^3\ arctg\left(\frac{U}{V}\right) + 12\,U\,WR - 18\,V^2\,W\log(R+U)) - 18\,V^2\,U\log(R+W) + 36\,U\,V\ \ W\log(R-V) + 18\,VW^2\ arctg\left(\frac{UV}{WR}\right) + 18\,V\,U^2 arctg\left(\frac{VW}{UR}\right) + 6W^3 log(R+U) + 6\,U^3 log(R+W) + 24\,V^2U - 6\,V^3\ arctg\left(\frac{UW}{RV}\right) + 18VVU^2\ \ arctg\left(\frac{W}{U}\right) + 36\,V\,W^2 arctg\left(\frac{U}{W}\right) + 18\,V\,W^2 arctg\left(\frac{W}{U}\right) - 54\,U\,V\,W - U^3) \quad (24)$$

II.3 MODIFIED FILAMENT METHOD

The filament method itself is an approximation technique where a conductor with a finite cross-section (like a coil wire) is modeled as one or more infinitesimally thin, current-carrying "filaments" or wires. This simplifies the complex 3D integration required by the Biot-Savart Law into more manageable 1D integrals. The modification involves regularizing the filament integrals (often by analytical or semi-analytical methods) to correctly account for the conductor's finite cross-section and avoid these unphysical singularities. Consider the two circular coils of rectangular cross section as shown in Figure 6 with currents I_1, I_2 flowing in primary and secondary coils. The cross-sectional area of the first coil of the mean radius r_p is divided into (2k+1) by (2N+1) cells, and that of the second of the mean radius r_s into (2m+1) by (2n+1) cells. Each cell in the first coil contains one filament, and the current density in the coil cross section is assumed to be uniform, so that the filament currents are equal [16].

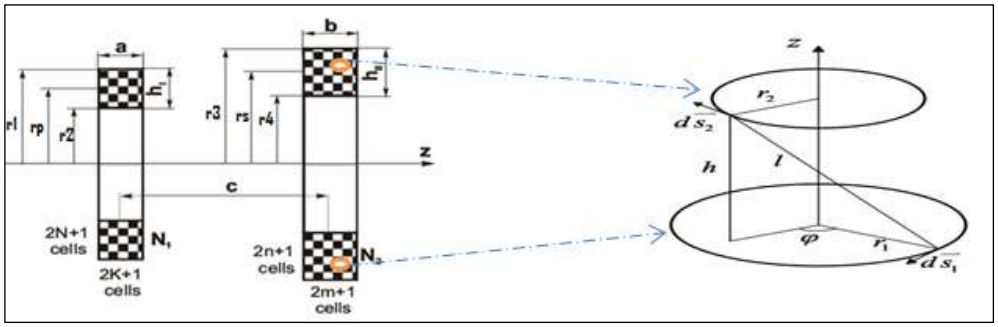

Figure 6: Configuration of mesh coils: two circular coils of rectangular cross section.
Source: Authors, (2025).

The expression for the mutual inductance between two coaxial filamentary circular coils of negligible cross-section is based on the use of Maxwell's coils and is given by the expression:

$$M = \frac{N_1 N_2 \sum_{g=-K}^{g=K} \sum_{h=-N}^{h=N} \sum_{p=-m}^{p=m} \sum_{l=-n}^{l=n} M(g,h,p,l)}{(2K+1)(2N+1)(2m+1)(2n+1)} \quad (25)$$

The formula for mutual inductance M(g,h,p,l) between two coaxial circular filamentary coils with radii r_s and r_p and separated by a distance d is given by:

$$M(g,h,l,p) = \frac{\mu_0}{\pi}\sqrt{r_s\, r_p}\int_0^{\pi} \frac{(cos(\theta) - \frac{d}{r_s} cos(\emptyset))\psi(k)}{\sqrt{V^3}}\, d\phi \quad (26)$$

Where

$$\psi(k) = \left(\frac{2}{k} - k\right) K(k) - \frac{2}{k} E(k) \quad (27)$$

$$V = \sqrt{1 - cos^2(\phi)\, sin^2(\theta) - 2\frac{d}{{r_s}^2} cos(\phi)\, cos(\theta) + \frac{d^2}{{r_s}^2}} \quad (28)$$

$$k^2 = \frac{4\alpha V}{(1+\alpha V)^2 + \xi^2} \quad (29)$$

$$r_p(h) = r_p + \frac{h_p}{(2N+1)} h, h = -N, \ldots, N \quad (30)$$

$$r_s(l) = r_s + \frac{h_s}{(2n+1)} l, l = -n, \ldots, n \tag{31}$$

$$z(g,p) = c - \frac{a}{(2K+1)} g + \frac{b\sin(\theta)}{(2m+1)} p, g = -K, \ldots, K, p = -m, \ldots, m \tag{32}$$

With

$$\xi = \beta - \alpha\cos(\phi)\sin(\theta), \alpha = \frac{r_s(l)}{r_p(h)}, \beta = \frac{z(g,p)}{r_1(h)}, r_s = \frac{r_3+r_4}{2}, h_s = r_3 - r_4 + r_w, r_p = \frac{r_1+r_2}{2}, h_s = r_1 - r_2 + r_w, y(p) = d + \frac{b\sin(\theta)}{(2m+1)} p, p = -m, \ldots, m \tag{33}$$

Where μ_o is the magnetic permeability of vacuum. K(k) and E(k) are the complete elliptic integral of the first kind and second kind, respectively. r_P is the radius of the primary coil; r_S is the radius of the secondary coil, c axial distance between coil midplanes, d radial distance between axes, a and b height of the primary coil and secondary coil, respectively. The electromagnetic force between two current-carrying coils with radial or axial misalignment can be derived from the general expression with their mutual inductance gradient. The force is calculated by the following equation:

$$F = I_1 I_2 \frac{\partial M}{\partial d} \tag{34}$$

Where I_1 and I_2 are the currents of two coils and d is the generalized coordinate. Applying some modification in the mutual inductance calculation, we deduced the magnetic force between the filamentary coils as follows:

- The propulsion magnetic force (axial force) for g = c:

$$F_{axial} = \frac{\mu_0 I_2 I_1}{2\pi\sqrt{\alpha}} \int_0^{\pi} \frac{(\frac{d}{r_2}\cos(\emptyset) - 1)\psi(k)}{\sqrt{V^5}} d\phi \tag{35}$$

- The restoring magnetic force (radial or lateral force) for g = d:

$$F_{radial} = \frac{\mu_0 I_2 I_1}{\pi\sqrt{\alpha}} \int_0^{\pi} \frac{(\frac{d}{R_S}\cos^2(\phi) + (1+\frac{d^2}{{R_S}^2))\ \cos(\phi) - 3\frac{d}{R_S})\chi(k)}{\sqrt{V^7}} d\phi + \frac{\mu_0 I_2 I_1}{\pi\alpha\sqrt{\alpha}} \int_0^{\pi} \frac{(1-\frac{d}{R_S}\cos(\phi))(\frac{d}{R_S} - \cos(\phi))\ \ (1+\beta^2-\alpha^2 V^2)\psi(k)}{\sqrt{V^9}} d\phi \tag{36}$$

Where

$$\psi(k) = k(\frac{2-k^2}{2(1-k^2)} K(k) - E(k)) \tag{37}$$

$$\chi(k) = \frac{1}{k}(\frac{2-k^2}{2} K(k) - E(k)) \tag{38}$$

IV. RESULTS AND DISCUSSIONS

To calculate the mutual inductance between two cylindrical magnets (or more accurately, two massive cylindrical coils carrying current, as shown in your diagrams), the most widely used and efficient approach involves the modified filament method or its semi-analytical variations. From the two magnets presented by the Amperian approach, we can calculate the magnetic force by the modified filament method. Consequently, in a first step, we have chosen to calculate the mutual inductance between cylindrical magnets as shown in Figure 7. For calculation purposes, the magnetization can be mathematically replaced by an equivalent volume current throughout its volume. This equivalent current is physically the same as that flowing in a coil, allowing the coil-based Biot-Savart Law to be used.

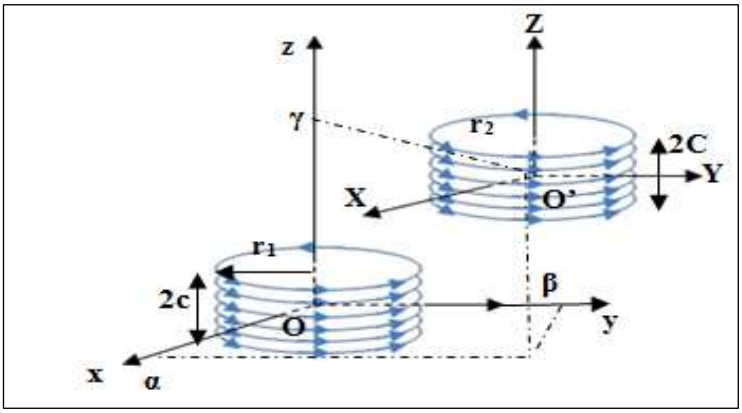

Figure 7: System of magnets to study.
Source: Authors, (2025).

Figure 8 is a representation of the mutual inductance between two coils/magnets versus the axial distance. The excellent match between the blue line (modified filament method) and the black circles (analytical solution) demonstrates that the modified filament method is highly accurate for calculating the mutual inductance of this specific coil configuration.

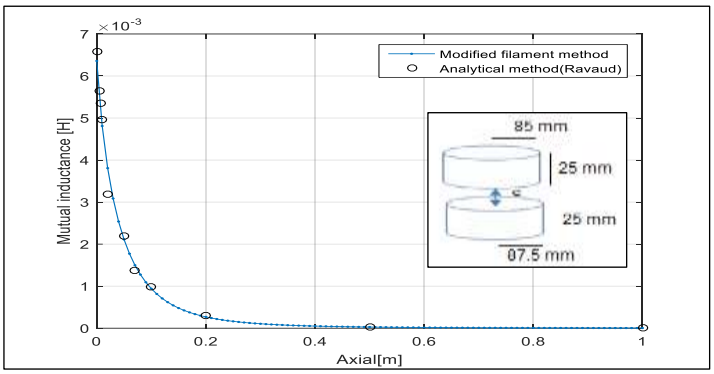

Figure 8: Representation of the mutual inductance between two magnets versus the axial.
Source: Authors, (2025).

As shown in Figure 3, the dimensions of the first elementary cuboidal magnet are a, b and c and its polarization is J. For the second elementary magnet, are A, B and C , its polarization is J' and the coordinate of its center is α, β and γ. The $\Delta x1_s$ and $\Delta x2_t$ are the width of the first and second elementary magnets. The upper magnet moves in translation along the y-axis above the lower fixed magnet. For comparing the result with our new approximation, we have calculated the same example (Figure 7) with modified filament method. In this example, as the magnetization J of the magnet PM1 and PM2 are perpendicular to the surfaces 2a x 2b and oriented to the top, its horizontal faces wear the density $\sigma = +J$on the upper face, and $\sigma = -J$ on the lower face. Calculating the exact magnitude of the radial force is mathematically complex, involving calculus and functions like elliptic integrals, especially for thick cylindrical magnets.

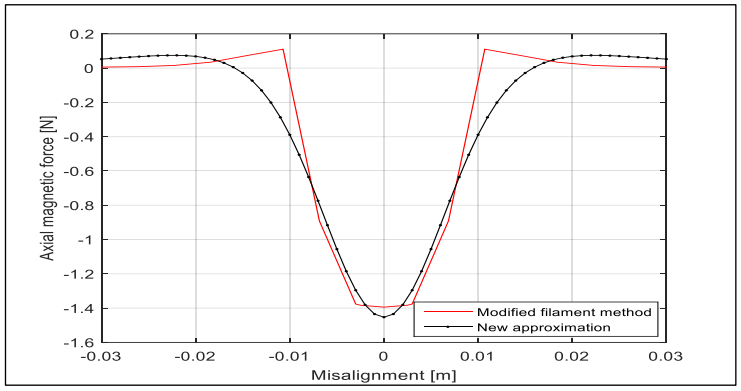

Figure 9: Force between magnets versus the misalignment axis (r_1=r_2=5mm, 2c=2C=10mm)
Source: Authors, (2025).

The takeaway from the Figure 9 is that both the "modified filament method" and the "new Approximation" yield results that are in remarkably good agreement across the range of radial misalignment, as indicated by the blue and red lines virtually overlapping. This suggests the "new Approximation" is a successful, and likely computationally less intensive, method for predicting the axial magnetic force in this system. The graph is demonstrating the sensitivity of the magnetic force to positional errors. Even small radial misalignments can significantly reduce the desired magnetic force (either attraction or repulsion) between the two cylindrical magnets. The Figure 10 is a cross-section of a voice coil motor, which is essentially an electromagnet designed to create motion. The VCM can provide very precise, continuous, and highly controlled motion, making it ideal for positioning and focusing applications.

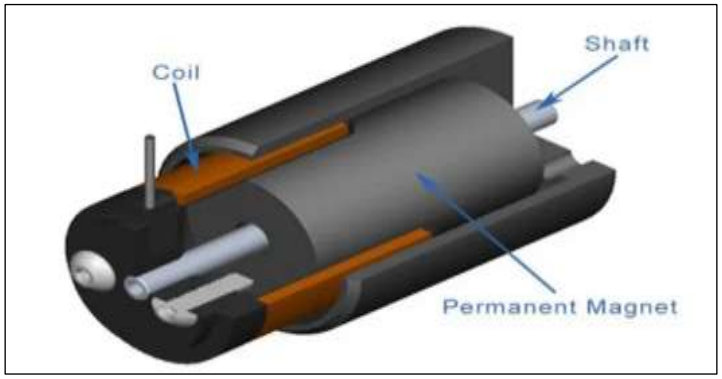

Figure 10: A cross-section of a voice coil motor
Source: Authors, (2025).

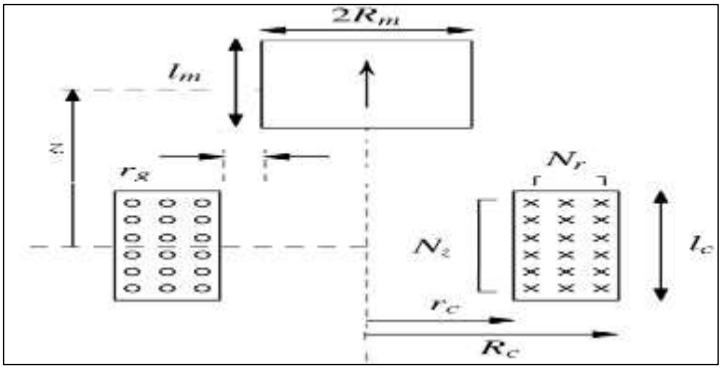

Figure 11: Geometrical parameters of the magnets-coil system
Source: Authors, (2025).

The Figure 11 is a diagram of an electromagnetic system, likely a simplified model for calculating magnetic forces or magnetic fields, such as those found in linear actuators, magnetic bearings, or electro-mechanical devices. It displays the geometric configuration and key dimensional parameters of a coil assembly interacting with a permanent magnet. The diagram features a permanent magnet at the top and a solenoid-like coil composed of multiple turns below, separated by an air gap. The axial separation is the key variable that changes the magnetic force. This geometrical model is typically used as the basis for analytical calculations of the axial magnetic force Fz between the magnet and the coil. The force will be a function of the axial separation, Fz(z), as well as the currents, dimensions, and magnetic properties of the materials. The Figure 12 purpose is to evaluate the accuracy of two computational methods ("modified filament method" and "new approximation") against actual experimental data ("measurement").

This figure is a plot comparing three different approaches for determining the axial magnetic force (measured in newtons, N) as a function of axial position (measured in meters, m). Both theoretical models generally follow the trend of the measured data. The modified filament method provides a very close fit to the measured data points, particularly in the initial range (0.016 m to 0.023). It consistently overestimates the force slightly compared to the measurements in the 0.023 to 0.026 m range, and does not show the peak and subsequent drop suggested by the measured data in the higher axial positions. The new approximation is most accurately captures the maximum force observed in the measured data (around 0.13 N at 0.0235 m). After the peak, it predicts a decrease in force, which aligns better with the general trend suggested by the few data points in the 0.024 m to 0.026 m range compared to the modified filament method. However, it seems to underestimate the force slightly in the initial range (0.016 m to 0.020 m). In summary, the graph illustrates the trade-offs in accuracy of the two computational models:

- The Modified filament method is generally very accurate but might not correctly predict the peak and subsequent drop in force.
- The new approximation is effective at modeling the peak force and subsequent decay but is less accurate at the lower axial positions.

For this case, the curves show good agreement between the approximation and the filament method results. Also, calculation results have been confirmed by measurement values (Figure 12). The measurement and simulation results are in very good agreement with calculation which indicates the feasibility of the approximation formulas.

Table 1: Design parameters for magnet-coil system

Dimensions	Quantity	Value
I	Coil current	0.2 A
R_c	Outer radius of primary coil	18 mm
r_c	Inner radius of primary coil	14 mm
L_c	Length of primary coil	10 mm
N_c	Number of turns of primary coil	120
Rm	Magnet radius	7.5 mm
B_r	Magnet remanence	1 T
L_m	Magnet length	10 mm

Source: Authors, (2025).

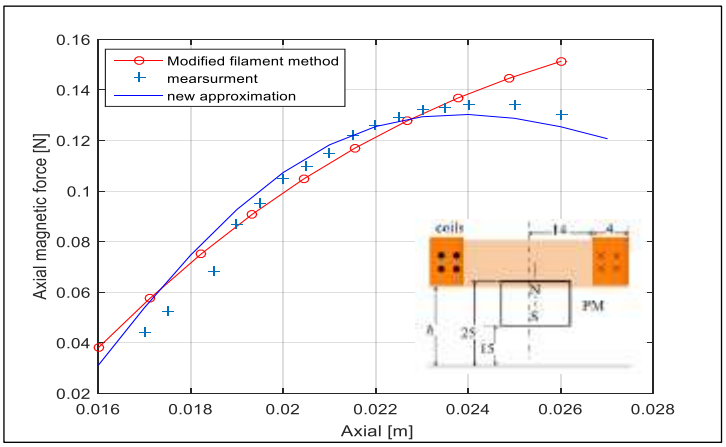

Figure 12: Axial force 'F_z 'obtained from measurement and our approximation in different positions

Source: Authors, (2025).

V. CONCLUSIONS

The paper introduces a new method for accurately calculating the magnetic force in two specific configurations: between two cylindrical permanent magnets and between a cylindrical permanent magnet and a large, circular coil (solenoid). The validity and accuracy of this new method were established by comparing its results against two established benchmarks: The modified filament method and measurement values. The new method was likely developed to offer a balance between the complexity of the highly accurate modified filament method and the need for fast, accurate calculation, possibly achieving high accuracy with fewer computational steps. The findings are highly relevant to the design and analysis of devices that use magnets and coils, such as magnetic bearings, linear motors, actuators, or energy harvesting systems. The results confirm that the forces calculated using the new approximation show "excellent agreement" with both the modified filament method and the actual experimental measurements.

VI. AUTHOR'S CONTRIBUTION

Conceptualization: Naamane Mohdeb, Hicham Allag and Mohammed Chebout.
Methodology: Hicham Allag and Naamane Mohdeb
Investigation: Naamane Mohdeb, Hicham Allag and Mohammed Chebout.
Discussion of results: Naamane Mohdeb, Hicham Allag and Mohammed Chebout.
Writing – Original Draft: Naamane Mohdeb
Writing – Review and Editing: Naamane Mohdeb and Mohammed Chebout.
Resources: Naamane Mohdeb and Mohammed Chebout.
Supervision: Hicham Allag, Mohammed Chebout and Naamane Mohdeb.
Approval of the final text: Hicham Allag, Naamane Mohdeb and Mohammed Chebout.

VII. ACKNOWLEDGMENTS

The authors of this article would like to thank the General Directorate of Scientific Research and Technological Development (DGRSDT) in Algeria for their technical support and the specific research budget allocated to this program.

VIII. REFERENCES

[1] V. Lemarquand, G. Lemarquand. : "Passive Permanent Magnet Bearings for Rotating Shaft: Analytical Calculation", Magnetic Bearings, Theory and Applications, Sciyo Published book, pp. 85-116, October 2010

[2] G. Akoun and J. P. Yonnet, "3D analytical calculation of the forces exerted between two cuboidal magnets," IEEE Transactions on Magnetics , vol. 20, no. 5, pp. 1962–1964, 1984.

[3] D. Vokoun, M. Beleggia, L. Heller and P. Sittner. "Magnetostatic interactions and forces between cylindrical permanent magnets". Journal of Magnetism and Magnetic Materials , vol. 321, pp.3758–3763, 2009

[4] H. Allag, J-P. Yonnet, M. Fassenet and M. E. H. Latrech, "3D analytical calculation of interactions between perpendicularly magnetized magnets—Application to any magnetization direction," Sensors Letters, vol. 7, no. 3, pp. 1–6, Jun. 2009

[5] Ravaud, R., G. Lemarquand, S. Babic, V. Lemarquand, and C. Akeyel. "Cylindrical magnets and coils: Fields, forces and inductances". IEEE Transactions on Magnetics , vol.46, pp.3585–3590. 2010.

[6] Ravaud, R., G. Lemarquand,& V. Lemarquand. Force and stiffness of passive magnetic bearings using permanent magnets. Part 2: Radial magnetization. IEEE Transactions on Magnetics, vol.45 pp.3334–3342. 2009.

[7] M. Hossein Partovi, Eliza J. Morris, "Eddy current damping of a magnet moving through a pipe," Canadian Journal of Physics. vol.84, pp.253–274 , 2006 .

[8] J. S. Agashe and D. P. Arnold, "Analytical force calculations and scaling effects for cylindrical and cuboidal micro-magnets," presented at the Intermag Conf., San Diego, CA, May 2006.

[9] E. P. Furlani, S. Reznik, and W. Jansen, "A three-dimensional field solution for bipolar cylinders," IEEE Transactions on Magnetics (IEEE), vol. 30, no. 5, pp. 2916–2919, Sep. 1994.

[10] E. P. Furlani, "Analytical analysis of magnetically coupled multipole cylinders," Journal of Physics D: Applied Physics, vol. 33, pp. 28–33, 2000.

[11] Furlani, E. P., S. Reznik, and A. Kroll. , "A three-dimensional field solution for radially polarized cylinders, ". IEEE Transactions on Magnetics, vol. 31, no.1, pp. 844–851,1995.

[12] N. Ivković, I, Jovanović, "Magnetic Field Calculation of a Permanent Ring Magnet with a Trapezoidal Cross-Section, ", 60th International Scientific Conference on Information, Communication and Energy Systems and Technologies (ICEST), North Macedonie, 2025.

[13] R.,G. Ravaud, V.Lemarquand and C. Depollier, "Analytical calculation of the magnetic field created by permanent-magnet rings," IEEE Trans. Magn.,Vol. 44,No. 8,1982–1989,Aug. 2008.

[14] Ravaud, R., G. Lemarquand, V. Lemarquand, and C. Depollier, "Discussion about the analytical calculation of the magnetic field created by permanent magnets," Progress In Electromagnetics Research B, vol. 11, 281-297, 2009.

[15] F. Xu, X. Xu and Z. Li, and Liang Chu, "Numerical Calculation of the Magnetic Field and Force in Cylindrical Single-Axis", IEEE Transactions on Magnetics Vol.50, pp1-6. 2014.

[16] Q. Wang, W. Che, M. Dionigi, F. Mastri, M. Mongiardo, and G. Monti, "Gains Maximization via Impedance Matching Networks for Wireless Power Transfer," Progress In Electromagnetics Research, Vol. 164, 135-153, 2019.

[17] S.I. Babic and C. Akyel. Calculating Mutual Inductance Between Circular Coils With Inclined Axes in Air. IEEE Transactions on Magnetics, 44(7):1743–1750, 2008.